ELSEVIER

PII: S0032-3861(96)00989-5

Polymer Vol. 38 No. 16, pp. 4103–4112, 1997

0032-3861/97/$17.00+0.00

Phase behaviour in binary mixtures of diblock copolymers as analysed by the random phase approximation calculations

Shinichi Sakurai* and Shunji Nomura
Department of Polymer Science and Engineering, Kyoto Institute of Technology, Matsugasaki, Sakyo-ku, Kyoto 606, Japan
(Received 3 July 1996; revised 20 September 1996)

Binary mixtures of diblock copolymers are interesting materials for controlling the size and the morphology of the microdomains in novel ways. We report here simulation results for the phase behaviour in binary mixtures of the diblock copolymers. The random phase approximation calculations were conducted for the binary mixtures of diblock copolymers, α: $(A-B)_1$ and β: $(A-B)_2$ to discuss stability of the homogeneous $(\alpha+\beta)$ mixture. The parameter values used for the simulations are that total degree of polymerization, $N(=N_\alpha=N_\beta)$, is 1000, the radius of gyration, $R_g(=R_{g,\alpha}=R_{g,\beta})$, is 10 nm, and the segmental volume, $v_A=v_B=100\,cm^3\,mol^{-1}$ for monodisperse and polydisperse samples $(1.0\leq M_w/M_n\leq 1.5)$. The fraction of A in $\alpha(f_A^\alpha)$ and that in $\beta(f_A^\beta)$ are varied in such a way to satisfy $f_A^\alpha+f_A^\beta=1$. As a result, it is predicted that the homogeneous mixture undergoes microphase separation as the segregation increases, for f_A^α larger than a particular value $(f_{A,crit}^\alpha)$ which is dependent on the values of M_w/M_n. On the other hand, for $f_A^\alpha<f_{A,crit}^\alpha$ the macroscopic phase separation between α and β is expected to occur prior to the microphase separation. It is also found that the wavelength of the dominant concentration fluctuation in the homogeneous mixture increases gradually as f_A^α approaches $f_{A,crit}^\alpha$ from the upper side of f_A^α. At $f_A^\alpha=f_{A,crit}^\alpha$, the wavelength diverges, indicating the macrophase separation. These results give some implications to the unit size of the microdomains formed upon the disorder-to-order transitions (ODT) for $f_A^\alpha>f_{A,crit}^\alpha$. Namely, the unit size might be larger than those of the component pure diblocks. The phase diagram of the ODT for the binary mixtures are found to depend on the compositions of α and β, i.e. the values of f_A^α and f_A^β. The phase boundary between the homogeneous (disordered) state and the microphase separated state for the binary mixture is found to be different from the one for the pure block copolymer. The result shows that the miscibility (disordered state) is suppressed in the binary mixture. © 1997 Elsevier Science Ltd.

(Keywords: binary mixtures of diblock copolymers; random phase approximation; microphase separation)

INTRODUCTION

Various studies of controlling morphology in block copolymers have been reported[1]. It is well known that the microdomain morphology is dependent on the composition of block copolymers. However, a synthetic technique is required for the control of the composition of a pure block copolymer. The situation is quite different from the case of polymer blends. To overcome such unfavourable factors, some conventional trials for controlling the microdomain morphologies have been conducted. One of these utilizes binary mixtures of block copolymer and homopolymer[2–8]. In principle, adding the homopolymer into the chemically identical microdomain of the block copolymer changes the effective volume fraction in the system, if homogeneous mixing is attained without macroscopic phase separation (*Figure 1a*). Moreover, another type of phase separation was found: localization of the homopolymers within the microdomain space, which is shown schematically in *Figure 1b*[2,9]. This is the case when comparatively long homopolymer chains are mixed, where very little interpenetration of the homopolymer chains into the block copolymer chains is shown, while macroscopic phase separation does not occur. However, a situation such as shown in *Figure 1b* makes the morphological control scheme complicated.

Recently, binary blends of block copolymers have attracted general interest in terms of their potential for controlling the size and the morphology of the microdomains in novel ways[2,8,10,11]. There were found experimentally[11] two representative states of phase separation in binary blends of block copolymers. One is macroscopic phase separation, and the other is homogeneous microphase separation, as shown schematically in *Figure 1c*. No intermediate states such as the localization found in the block copolymer/homopolymer blends may be considered for binary blends of the block copolymers. Therefore, as a conventional morphological control, binary blends of block copolymers may be more suitable than the block copolymer/homopolymer blends. Some experimental studies have already been conducted to examine miscibility and phase structures in binary blends of polystyrene-*block*-polyisoprene (SI) diblock copolymers[11–13]. Moreover, some theoretical studies have shown that the self-consistent field (SCF) theory is useful to examine phase behaviour and the morphological structures of binary blends of diblock copolymers[14–18].

It is of great interest to examine whether the same morphologies can be obtained if the average compositions

* To whom correspondence should be addressed

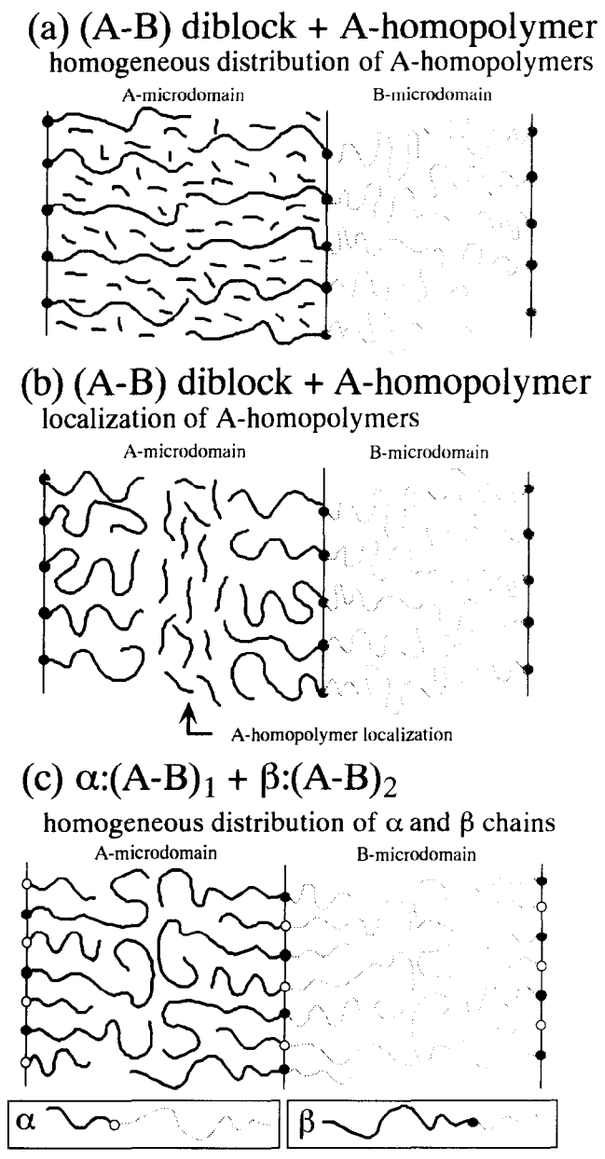

Figure 1 Schematic representation of the distribution of polymer chains in the microdomain structures. (a) Mixture of A–B diblock copolymers with relatively short A-homopolymers showing comparatively homogeneous distributions of the A-block and A-homopolymer chains. (b) Mixture of A–B diblock copolymers with comparatively long A-homopolymers showing localization of the A-homopolymers in the A-microdomains. (c) Binary mixtures of diblock copolymers, α: $(A-B)_1$ and β: $(A-B)_2$. Homogeneous distributions of the A and B chains in the respective domains are sketched

are matched to the pure block copolymers. For this purpose, the phase diagram has been checked both theoretically[18] using the SCF theory and experimentally[19]. The results indicated that exactly the same morphological state was not obtained. There are plenty of molecular parameters and combinations which should be focused on in order to highlight the difference. Some systematic studies have been conducted on pairs with the same compositions (~50/50, lamellae) but different molecular weights[12,16,17], and on pairs with the same molecular weights but different compositions[15,18]. The system that we deal with in this paper is the particular case of the latter pairs. Namely, the fraction of A in $\alpha(f_A^{\alpha})$ and that in $\beta(f_A^{\beta})$ are varied in such a way to satisfy $f_A^{\alpha} + f_A^{\beta} = 1$ [α: $(A-B)_1$ and β: $(A-B)_2$]. We focus exclusively on the total average of 50/50 composition with lamellar structures. First of all, we examine whether the macroscopic or microscopic phase separation occurs preferentially when the homogeneous mixture of the block copolymers in the disordered state is quenched into the weak segregation regime. Then, we evaluate the size of the structure developed upon the disorder-to-order transition (ODT) by stability analysis using random phase approximation (RPA) calculations[20–22]. Using SCF theory, Shi and Noolandi[15] have presented a great deal of similar results which we present hereafter. The significance of our study using the RPA theory is that we can calculate scattering functions and can evaluate the size of the dominant concentration fluctuation in the homogeneous mixture of diblocks. The results may have implications for the phase structures in the weak segregation regime, which are formed upon the ODT and even may affect the following structural development. In the case of the solution cast for the sample film preparation, the situation that the segregation becomes stronger as the solvent evaporates is similar to that considered in the present paper, and, thus, the resultant structures may be different from those predicted for the strong segregation regime.

The shortcoming that we can hardly change the composition of the pure block copolymers also induces retardation of experimental studies on the composition dependence of the interaction parameter for the pure block copolymers. As well as the above, utilizing the binary mixtures of the block copolymers may be a candidate for the conventional strategies. Of course, the present situation is a completely homogeneous mixture of those copolymers in the disordered state. We usually evaluate the interaction parameter by analysing the elastic scattering from the disordered state using RPA calculations. It is to be expected that the scattering function for binary mixtures of block copolymers differs from that for the pure block copolymer. In order to examine the difference in the scattering function for a given value of the interaction parameter, we also conducted RPA calculations. We also discuss the difference in the phase diagram for the ODT between the pure block copolymer and the binary mixture of the block copolymers.

THEORETICAL BACKGROUND

The elastic scattering is ascribed to the concentration fluctuation in the disordered state, which can be expressed by the RPA as;

$$I(q) = K(a-b)^2\left[\frac{S(q)}{W(q)} - 2\chi\right]^{-1} \tag{1}$$

with

$$S(q) = S_{AA}(q) + 2S_{AB}(q) + S_{BB}(q) \tag{2}$$

and

$$W(q) = S_{AA}(q)S_{BB}(q) - \{S_{AB}(q)\}^2 \tag{3}$$

where q is the magnitude of the scattering vector, defined as;

$$q = (4\pi/\lambda)\sin(\theta/2) \tag{4}$$

with θ and λ being the scattering angle and the

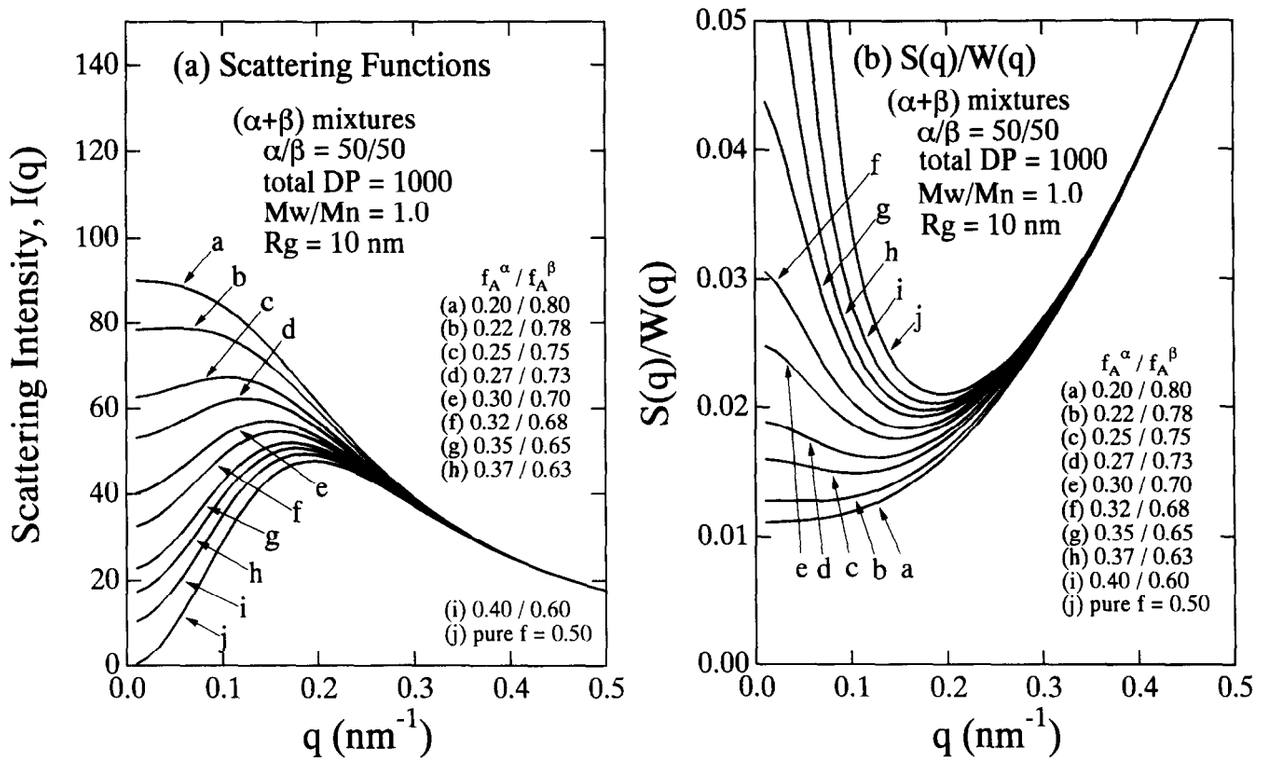

Figure 2 (a) Scattering functions for binary mixtures of diblock copolymers, α: $(A-B)_1$ and β: $(A-B)_2$ at $\chi = 0$. (b) $S(q)/W(q)$ as a function of q, where q denotes the magnitude of the scattering vector [see equation (4)]. The fraction of A in $\alpha(f_A^{\alpha})$ and that in $\beta(f_A^{\beta})$ are varied in such a way to satisfy $f_A^{\alpha} + f_A^{\beta} = 1$. The blend ratio is fixed at $\alpha/\beta = 50/50$, so as to fix the total fraction of A at 0.5. The parameter values used for the random phase approximation calculations are such that the total degree of polymerization, $N(=N_{\alpha} = N_{\beta})$, is 1000, the radius of gyration, $R_g(=R_{g,\alpha} = R_{g,\beta})$, is 10 nm, the inhomogeneity index of molecular weight, M_w/M_n, is 1.0, and the segmental volume, $v_A = v_B = 100\,\mathrm{cm^3\,mol^{-1}}$

wavelength of radiation, respectively. K is a proportional constant, a and b are the electron densities of the A and B segments, respectively, and χ is the interaction parameter between the A and B segments. The correlation functions $S_{AA}(q)$, $S_{BB}(q)$, and $S_{AB}(q)$ in equations (2) and (3) are given for A–B type diblock copolymers as follows;

$$S_{AA}(q) = r_C f_A^2 g_A^{(2)}(q) \tag{5}$$

$$S_{BB}(q) = r_C f_B^2 g_B^{(2)}(q) \tag{6}$$

$$S_{AB}(q) = r_C f_A f_B g_A^{(1)}(q) g_B^{(1)}(q) \tag{7}$$

with the reduced degree of polymerization, r_C, for the entire diblock copolymer, which is defined as;

$$r_C = (v_A N_A + v_B N_B)/v_0 \tag{8}$$

and, thus, the fraction of the K component, f_K, is given by

$$f_K = r_K/r_C = v_K N_K/(v_A N_A + v_B N_B) \tag{9}$$

v_K and v_0 denote the molar volume of the K segment and that of the reference cell, respectively. v_K is actually calculated with $v_K \equiv M_{u,K}/\rho_K$, where $M_{u,K}$ is a molecular weight of the K segment, and ρ_K is the mass density of the K polymer (K = A or B). We assumed $v_0 = (v_A v_B)^{1/2}$. The volume-average single chain correlation functions, $g_K^{(1)}(q)$ and $g_K^{(2)}(q)$ in equations (5)–(7) are given by;

$$g_K^{(1)}(q) = \frac{1}{x_K}\left[1 - \left\{\frac{1}{x_K(\lambda_K - 1) + 1}\right\}^{1/(\lambda_K - 1)}\right] \tag{10}$$

$$g_K^{(2)}(q) = \frac{2}{x_K^2}\left[x_K - 1 + \left\{\frac{1}{x_K(\lambda_K - 1) + 1}\right\}^{1/(\lambda_K - 1)}\right] \tag{11}$$

for the Gauss chain using Schultz–Zimm's molecular weight distribution function[23,24]. Note that the second term in the square brackets [...] of equation (10) and the third term in [...] of equation (11) converge on $\exp(-x_K)$ for the monodisperse limit. Namely, equation (11) is identical to the Debye function in the limit, where x_K is defined by;

$$x_K = N_K b_K^2 q^2/6 \tag{12}$$

with b_K being the statistical segment length for the K polymer (K = A or B). In equations (10) and (11), λ_K characterizes polydispersity of the K-block chain in the diblock copolymer, i.e. $\lambda_K \equiv (M_w/M_n)_K$. Since the values of λ_K are not always individually available, we calculated λ_K from the polydispersity index for the entire diblock copolymer, $M_w/M_n(\equiv\lambda_0)$, using the relationship expressed by equation (13) assuming $\lambda_A = \lambda_B$;

$$\lambda_0 - 1 = (\lambda_A - 1)w_A^2 + (\lambda_B - 1)w_B^2 \tag{13}$$

with w_A and w_B being the weight fractions of A and B, respectively.

To calculate the scattering function for the binary mixture of the diblock copolymers in the disordered state, we have only to modify the correlation functions S_{AA}, S_{BB} and S_{AB} by volume averaging

as follows;

$$S_{AA}(q) = \phi_\alpha S^\alpha_{AA}(q) + \phi_\beta S^\beta_{AA}(q) \quad (14)$$

$$S_{BB}(q) = \phi_\alpha S^\alpha_{BB}(q) + \phi_\beta S^\beta_{BB}(q) \quad (15)$$

$$S_{AB}(q) = \phi_\alpha S^\alpha_{AB}(q) + \phi_\beta S^\beta_{AB}(q) \quad (16)$$

where ϕ_α and ϕ_β denote the fractions of α and β in the $(\alpha+\beta)$ mixture, respectively $(\phi_\alpha + \phi_\beta = 1)$. $S^\alpha_{AA}(q)$ expresses A–A correlation in the α block, and similar notations for the other pair correlations.

RESULTS AND DISCUSSION

Figure 2a shows the simulated scattering functions, $I(q)$ vs q, for binary mixtures of diblock copolymers, α: $(A-B)_1$ and β: $(A-B)_2$ at $\chi = 0$. The fraction of A in $\alpha(f^\alpha_A)$ and that in $\beta(f^\beta_\beta)$ are varied so that $f^\alpha_A + f^\beta_A = 1$. The blend ratio is fixed at $\alpha/\beta = 50/50$, so as to fix the total fraction of A $(\overline{f_A})$ at 0.5. The parameter values used for the simulations are that the total degree of polymerization, $N(=N_\alpha = N_\beta)$, is 1000, the radius of gyration, $R_g(=R_{g,\alpha} = R_{g,\beta})$, is 10 nm, the inhomogeneity index of molecular weight, M_w/M_n, is 1.0, and the segmental volume, $v_A = v_B = 100\,cm^3\,mol^{-1}$. Since the scattering function is unaffected by an exchange of A and B notations for those parameters, we restricted the calculation of the scattering functions and further discussion of the results to $f^\alpha_A \leq 0.5$ $(f^\beta_A \geq 0.5)$. For most cases, a single peak is observed due to the *correlation hole effect*[20,21]. It is clearly observed that the peak shifts towards smaller q-region with the peak intensity increasing as f^α_A approaches 0.20. For $f^\alpha_A = 0.20$, the scattering function has no peak at a finite non zero q-value. Another characteristic feature is the non zero intensity at $q = 0$ for the $(\alpha+\beta)$ mixtures. It is quite opposed to the pure block copolymer which has zero scattering intensity at $q = 0$, as seen in *Figure 2a* for the pure block copolymer with an A fraction of 0.5. This indicates that the concentration fluctuation having infinite wavelength is induced due to blending of diblock copolymers α and β which have different compositions. These features are characteristic of the block copolymers having wide molecular weight and composition distributions, which have been already reported[25–27]. According to equation (1), it is expected that the peak intensity becomes more intense as χ approaches the spinodal value (χ_S) from $\chi = 0$, and that it diverges at $\chi = \chi_S$, where χ_S is given by

$$\chi_S = \frac{1}{2}\frac{S(q_m)}{W(q_m)} \quad (17)$$

with q_m being the q-value of the peak. χ_S should read $\chi_{s,Macro}$ and $\chi_{s,ODT}$ for $q_m = 0$ and for $q_m \neq 0$, respectively. Here $\chi_{s,Macro}$ and $\chi_{s,ODT}$ designate spinodal χ values for the macroscopic phase separation and the ODT (microphase separation), respectively. Therefore, the fact that the scattering function has no peak at a finite non zero q-value for $f^\alpha_A \lesssim 0.20$ indicates that macroscopic phase separation occurs preferentially in the $(\alpha+\beta)$ mixtures when the homogeneous $(\alpha+\beta)$ mixtures in the disordered state are brought into the weak segregation regime. On the other hand, the microphase separation proceeds for $f^\alpha_A > 0.20$. In order to evaluate numerically those spinodal χ values, we should examine the behaviour of $S(q)/W(q)$ as a function of q. The plot is shown for various $(\alpha+\beta)$ mixtures in *Figure 2b*. It is again confirmed that the macrophase separation occurs preferentially when $f^\alpha_A \lesssim 0.20$ and the microphase separation proceeds first for $f^\alpha_A > 0.20$. $\chi_{s,Macro}$ and $\chi_{s,ODT}$ can be evaluated for $f^\alpha_A \lesssim 0.20$ and for $f^\alpha_A > 0.20$, respectively, using the minimum value of $S(q)/W(q)$*. The simulated results imply that we can obtain homogeneous microdomains without macrophase separation in the binary blends of diblock copolymers if those compositions are not too different $(f^\alpha_A > 0.20)$. Here, homogeneous microdomains for the binary blends mean that the K-block chains of α and β are homogeneously displaced in the K-microdomain space (K = A or B), as schematically represented in *Figure 1c*.

As for the case when those block copolymers have molecular weight distributions, the results change slightly. *Figure 3* shows the same plots as *Figure 2*. Here, $M_w/M_n = 1.1$, while the other parameter values are identical to those used for *Figure 2*. One of the big differences is non zero intensity at $q = 0$ even for the pure block copolymer with the A fraction of 0.5. In this case, the concentration fluctuation having infinite wavelength can be ascribed to molecular weight distribution and composition distributions[25–27]. In other words, the copolymers with those distributions should be considered to be multi-component mixtures. Another big difference is that the critical value of f^α_A for the border $(f^\alpha_{A,crit})$ between the macrophase separation and the ODT shifts towards the larger values $(f^\alpha_{A,crit} \cong 0.25)$, as compared to that for $M_w/M_n = 1.0$. We will discuss this fact later on in *Figure 4*. For $M_w/M_n = 1.1$, $\chi_{s,Macro}$ and $\chi_{s,ODT}$ are also evaluated from the minimum values of $S(q)/W(q)$*. The plots of $S(q)/W(q)$ are shown in *Figure 3b* for $M_w/M_n = 1.1$.

Plots of $\chi_{s,Macro}\overline{r_C}$ and $\chi_{s,ODT}\overline{r_C}$ vs f^α_A for the $(\alpha+\beta)$ mixtures are shown in *Figure 4a* for $M_w/M_n = 1.0$–1.5. Here, $\chi_{s,Macro}\overline{r_C}$ designates a product of $\overline{r_C}$ and the spinodal χ value at the macrophase separation. $\overline{r_C}$ is the volume averaged r_C for the $(\alpha+\beta)$ mixture, defined as;

$$\overline{r_c} = \phi_\alpha r^\alpha_c + \phi_\beta r^\beta_c \quad (18)$$

where r^α_C and r^β_C denote the reduced degrees of polymerization for the α and β chains, respectively. Similarly, $\chi_{s,ODT}\overline{r_C}$ stands for a product of $\overline{r_C}$ and the spinodal χ value at the ODT. Note here again that the blend ratio is fixed at $\alpha/\beta = 50/50$, so as to fix the total fraction of A at 0.5. The full and broken curves are for $\chi_{s,ODT}\overline{r_C}$ and $\chi_{s,Macro}\overline{r_C}$, respectively. Note that the value of $\chi_{s,ODT}\overline{r_C}$ is equal to 10.5 for the pure monodisperse block copolymer having the A fraction of 0.5, which is well known as the critical point first reported by Leibler[20]. It is also noted that $\chi_{s,Macro}\overline{r_C} = 2.0$ at $f^\alpha_A = 0$ for the monodisperse sample, being consistent with the critical value for a symmetric A/B homopolymer mixture at the critical concentration of 50/50[21]. For a given value of M_w/M_n, $\chi_{s,ODT}\overline{r_C}$ and $\chi_{s,Macro}\overline{r_C}$ decrease with a decrease of f^α_A

* For $f^\alpha_A > f^\alpha_{A,crit}$, the $S(q)/W(q)$ has a finite value at $q = 0$. This indicates that we can determine $\chi_{s,Macro}$ as well as $\chi_{s,ODT}$, although $\chi_{s,Macro} > \chi_{s,ODT}$. That is, there may be a chance for the sample to undergo macrophase separation. However, the fact of $\chi_{s,Macro} > \chi_{s,ODT}$ means that the microphase separation proceeds preferentially. Therefore, the prediction of the macrophase separation which is for the homogeneous $(\alpha+\beta)$ mixtures would lack the applicability to the samples already microphase separated

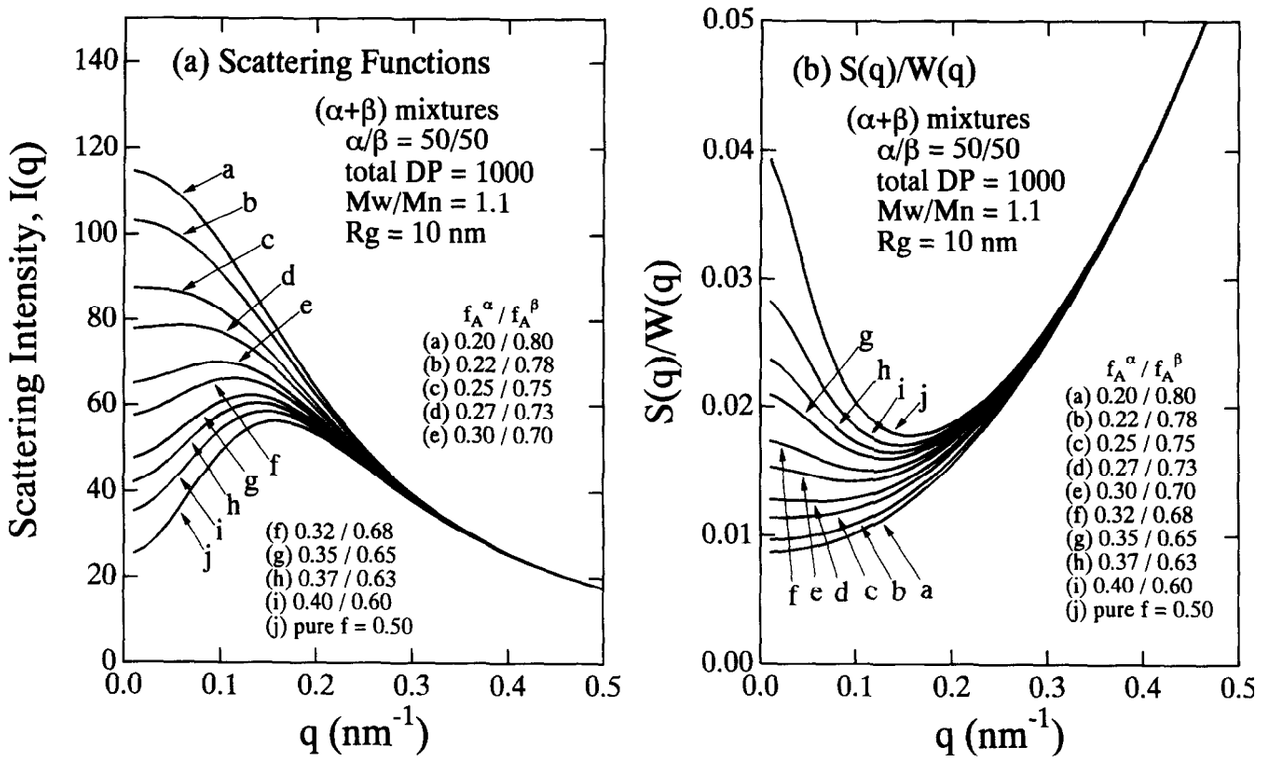

Figure 3 Similar plots as those in *Figure 2*. Here, the value of $M_w/M_n = 1.1$ is used, and the other parameter values are the same as those for *Figure 2*

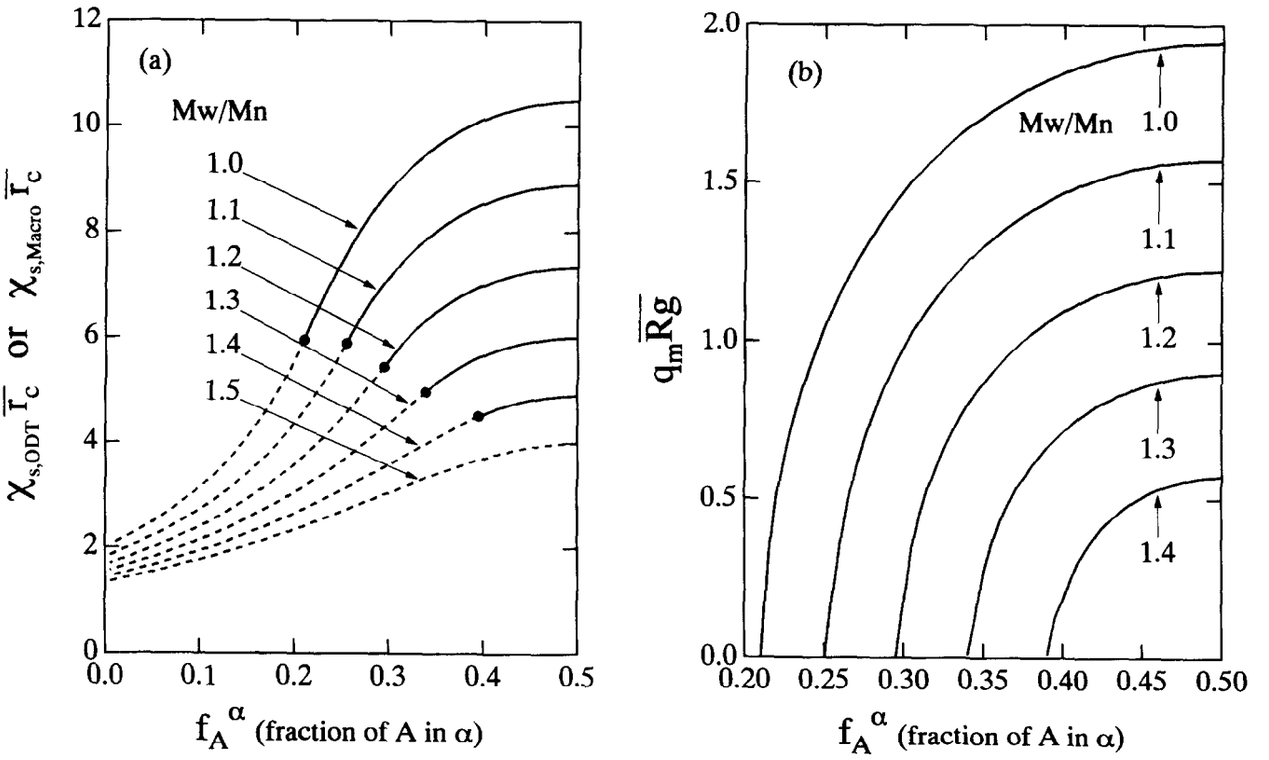

Figure 4 (a) Plots of $\chi_{s,ODT}\overline{r_C}$ and $\chi_{s,Macro}\overline{r_C}$ vs f_A^α for the binary mixtures of diblock copolymers, α: $(A-B)_1$ and β: $(A-B)_2$. Here, $\chi_{s,ODT}\overline{r_C}$ designates a product of $\overline{r_C}$ [volume averaged r_C for the $(\alpha+\beta)$ mixture, see equation (18)] and the spinodal χ value at the ODT, and $\chi_{s,Macro}\overline{r_C}$ is a product of $\overline{r_C}$ and the spinodal χ value at the macrophase separation. f_A^α is the fraction of A in α. The blend ratio is fixed at $\alpha/\beta = 50/50$, so as to fix the total fraction of A at 0.5. The full and broken curves are for $\chi_{s,ODT}\overline{r_C}$ and $\chi_{s,Macro}\overline{r_C}$, respectively. The closed circles are the border ($f_{A,crit}^\alpha$) between the macrophase and the microphase separations. (b) Plots of $q_m\overline{R_g}$ vs f_A^α for the $(\alpha+\beta)$ mixtures. $q_m\overline{R_g}$ is a product of q_m (the peak position of the scattering function in the disordered state) and $\overline{R_g}$ [volume averaged R_g for the $(\alpha+\beta)$ mixture]

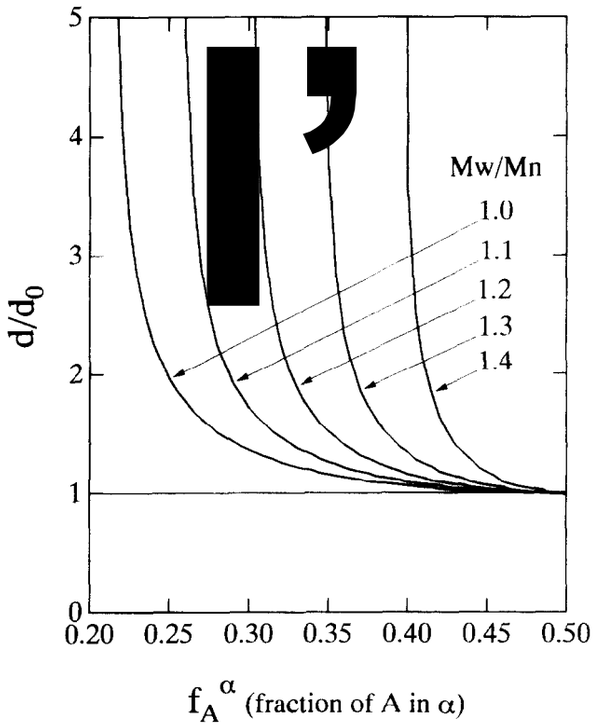

Figure 5 Plots of the ratio d/d_0 vs f_A^α, where d and d_0 denote, respectively, the wavelength of the dominant concentration fluctuation for the $(\alpha+\beta)$ mixtures and that for the pure α or β. d and d_0 are defined as $2\pi/q_m$ with q_m being the q value of the peak in the scattering function from the disordered state

and the shape of those f_A^α-dependencies is sigmoidal. Namely, the $(\alpha+\beta)$ mixture becomes less miscible as the asymmetry in the compositions of α and β increases. For a given f_A^α the values of $\chi_{s,ODT}\overline{rC}$ and $\chi_{s,Macro}\overline{rC}$ become smaller as M_w/M_n increases, because of the effect of multi-component blend for the polydisperse samples. The critical f_A^α values ($f_{A,crit}^\alpha$) for the border between the macrophase and microphase separations are shown with closed circles in *Figure 4a*. It is clearly seen that $f_{A,crit}^\alpha$ increases with an increase of the value of M_w/M_n. On the other hand, the $\chi_{s,ODT}\overline{rC}$ value at $f_A^\alpha = f_{A,crit}^\alpha$ decreases with an increase of M_w/M_n.

Figure 4b shows the plots of $q_m\overline{R_g}$ vs f_A^α for the $(\alpha+\beta)$ mixtures. The blend ratio is fixed at $\alpha/\beta = 50/50$, so as to fix the total fraction of A at 0.5. Here, $q_m\overline{R_g}$ is a product of q_m and $\overline{R_g}$ (volume averaged R_g for the $(\alpha+\beta)$ mixture with the definition similar to the equation (18)), where q_m is the peak position of the scattering function in the disordered state and indicates the wavenumber of the dominant concentration fluctuation which first diverges upon the ODT. In other words, we can evaluate the characteristic size of the domains first formed when the samples are subjected to the weak segregation regime from the disordered state. It is clearly observed that the $q_m\overline{R_g}$ value first decreases gradually and then decreases abruptly with a decrease of f_A^α. The value continuously decreases to zero at $f_A^\alpha = f_{A,crit}^\alpha$. Note here that there is no gap in $q_m\overline{R_g}$ in the vicinity of the border ($f_A^\alpha \approx f_{A,crit}^\alpha$). This results give us a quite interesting indication that by blending the binary diblock copolymers the characteristic size of the microdomains can be much larger than those of the component pure blocks. Moreover, the size may become quasi-macroscopic, i.e. we would have very large-size microphase-separated structures! However, it may not be possible to have a quite large size of the microdomain. We discuss the phase structures formed from such a concentration fluctuation upon the ODT later.

In order to demonstrate the wavelength of the concentration fluctuation in the binary mixtures definitely becomes much larger than that in the pure α or β component†, the ratio d/d_0 is shown as a function of f_A^α in *Figure 5*, where d and d_0 denote, respectively, the characteristic length of the fluctuation for the $(\alpha+\beta)$ mixtures and for the pure α or β. d and d_0 are defined as $2\pi/q_m$ with q_m being the q value of the peak in the scattering function from the disordered state. The ratio d/d_0 diverges at $f_A^\alpha = f_{A,crit}^\alpha$. For the monodisperse ($M_w/M_n = 1.0$) or almost monodisperse ($M_w/M_n = 1.1-1.2$) sample, we may obtain a sufficiently large f_A^α range for controlling the wavelength for $d/d_0 \lesssim 2.0$.

Finally, the phase diagram (plot of $\chi_{s,ODT}\overline{rC}$ vs total fraction of $A(\overline{f_A})$) is examined for the binary mixtures of the diblock copolymers to demonstrate how it is different from the phase diagram for the pure block copolymer. The parameter values used for the RPA calculations are so that the total degree of polymerization, $N(=N_\alpha = N_\beta)$, is 1000, the radius of gyration, $R_g(=R_{g,\alpha} = R_{g,\beta})$, is 10 nm, the inhomogeneity index of molecular weight, M_w/M_n, is 1.0, and the segmental volume, $v_A = v_B = 100\,cm^3\,mol^{-1}$. Here, $f_A^\alpha = 0.21$ and $f_A^\beta = 0.79$ were used. The blend ratio α/β is varied to control $\overline{f_A}$. The resultant phase diagram is presented in *Figure 6a*. The thick full curve is for the ODT and the broken curve is for the macrophase separation ($\chi_{s,Macro}\overline{rC}$). In the vicinity of $\overline{f_A} = 0.5$, only the macrophase separation is predicted. The parameter region of $\overline{f_A}$ for the macrophase separation can be clearly extracted from the plot of $q_m\overline{R_g}$ (shown in *Figure 6b*) with $q_m\overline{R_g} = 0$. On the other hand, both the macrophase and microphase separations are predicted in the region besides $\overline{f_A} \cong 0.5$, where $\chi_{s,ODT}\overline{rC} < \chi_{s,Macro}\overline{rC}$. However, the microphase separation preferentially proceeds for this region. Therefore, the prediction of the macrophase separation for the homogeneous $(\alpha+\beta)$ mixture at the broken curve is no longer applicable, because the sample is already microphase separated. The thin full curve is for $\chi_{s,ODT}\overline{rC}$ in the pure block copolymer. The disagreement in $\chi_{s,ODT}\overline{rC}$ between the pure block copolymer and the $(\alpha+\beta)$ mixture is pronounced in almost the entire region of $\overline{f_A}$ besides the vicinity of $\overline{f_A} = f_A^\alpha$ or $\overline{f_A} = f_A^\beta$. Namely, the miscibility (disordered state) is suppressed in the binary mixture. This should be borne in mind for the experiments, for example, in the case of the study of the composition dependence of the interaction parameter. The binary mixture cannot provide a conventional way as an alternative to the pure block copolymer. In other words, the results for the composition dependence of the interaction parameter χ evaluated from the $(\alpha+\beta)$ mixtures may be different from those of the pure block copolymers. The dependencies of $q_m\overline{R_g}$ on $\overline{f_A}$ are shown in *Figure 6b*. It is noteworthy again that $q_m\overline{R_g}$ changes drastically with $\overline{f_A}$ for the $(\alpha+\beta)$ mixtures, while there is

† Note that the pure α and β components give the same scattering function since it is unaffected by an exchange of A and B notations for this particular case with $f_A^\alpha = 1 - f_A^\beta$

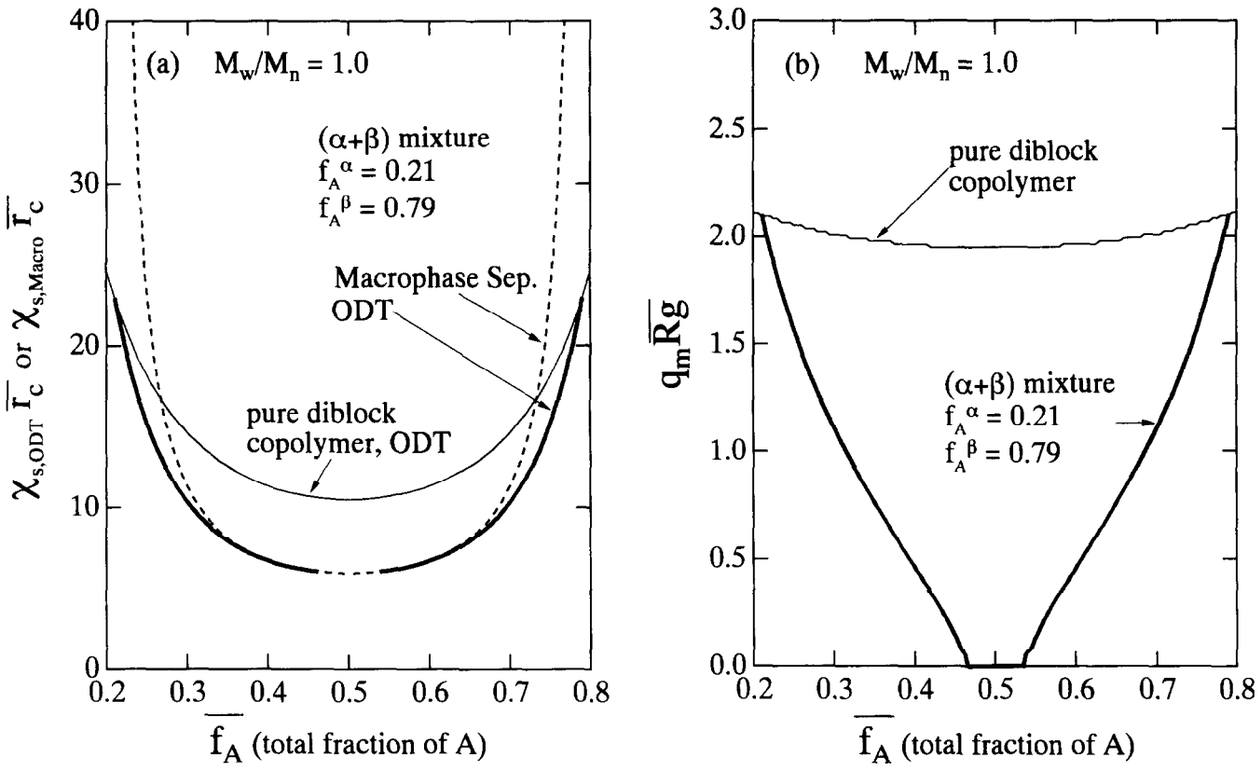

Figure 6 (a) Plots of $\chi_{s,ODT}\overline{r_C}$ and $\chi_{s,Macro}\overline{r_C}$ vs total fraction of A ($\overline{f_A}$) for the binary mixtures of diblock copolymers, α with $f_A^\alpha = 0.21$ and β with $f_A^\beta = 0.79$. The blend ratio α/β is varied to control $\overline{f_A}$. The thick full curve is for the ODT and the broken curve is for the macrophase separation. The thin curve is for $\chi_{s,ODT}\overline{r_C}$ for the pure block copolymer. The parameter values used for the random phase approximation calculations are that total degree of polymerization, $N(=N_\alpha = N_\beta)$, is 1000, the radius of gyration, $R_g(=R_{g,\alpha} = R_{g,\beta})$, is 10 nm, the inhomogeneity index of molecular weight, M_w/M_n, is 1.0, and the segmental volume, $v_A = v_B = 100\,cm^3\,mol^{-1}$. (b) Plots of $q_m\overline{R_g}$ as a function of $\overline{f_A}$ for the $(\alpha+\beta)$ mixtures, corresponding to (a)

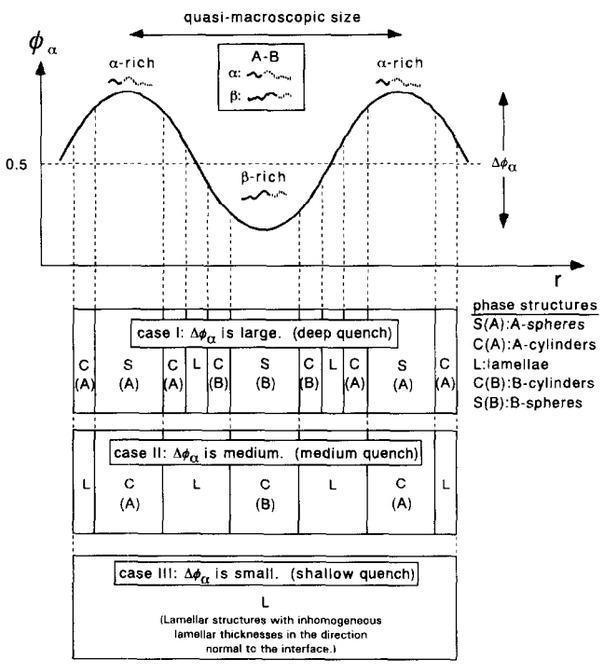

Figure 7 Schematic illustrations for the concentration fluctuation with a quasi-macroscopic wavelength and for the phase structures formed upon the disorder-to-order transition. Note that the wavelength is quasi-macroscopic so that the α- or β-rich regions are much larger than the chain dimensions of the diblocks. ϕ_α is the fraction of the α component, and $\Delta\phi_\alpha$ is the difference in ϕ_α between the α- and β-rich regions. The phase structures are shown in the three particular cases in terms of $\Delta\phi_\alpha$, where S(A), C(A), L, C(B), and S(B) denote A-spheres, A-cylinders, lamellae, B-cylinders, and B-spheres, respectively

trivial dependence of $q_m\overline{R_g}$ on $\overline{f_A}$ for the pure diblock copolymer, $q_m\overline{R_g}$ varying at around 2.0.

Implications for the phase structures

Figure 7 shows schematically the concentration fluctuation with a quasi-macroscopic wavelength, where the ordinate is for the fraction of the α component, ϕ_α. Note that the wavelength is quasi-macroscopic so that the α- or β-rich regions are much larger than the chain dimensions of the diblocks. With this situation, we consider formation of the phase structures upon the ODT for the three particular cases in terms of $\Delta\phi_\alpha$ (the difference in ϕ_α between the α- and β-rich regions). When $\Delta\phi_\alpha$ is large (case I), which corresponds to deep quench, the α- and β-rich regions transform into grains with A- and B-spherical domains, respectively. According to the periodic displacement of the α- and β-rich regions in the disordered state, the resultant grains with A- and B-spherical domains may be placed with a roughly constant distance. Such a feature has been confirmed experimentally for the blends of SI's[13]. There is a chance to see cylindrical and lamellar phases in between those grains, where the local average of the A fraction changes from f_A^α to f_A^β through 0.5. Thus, the phase structures may be what we depict in the case I. The same consideration for the blend of cylinder-forming diblocks has been presented by Hashimoto *et al.*[2]. For a medium $\Delta\phi_\alpha$ (case II, medium quench), the α- and β-rich regions contain an amount of β and α chains, therefore, those regions transform into A- and B-cylindrical grains, respectively, as shown in case II. For case III where $\Delta\phi_\alpha$ is small (shallow quench), the average

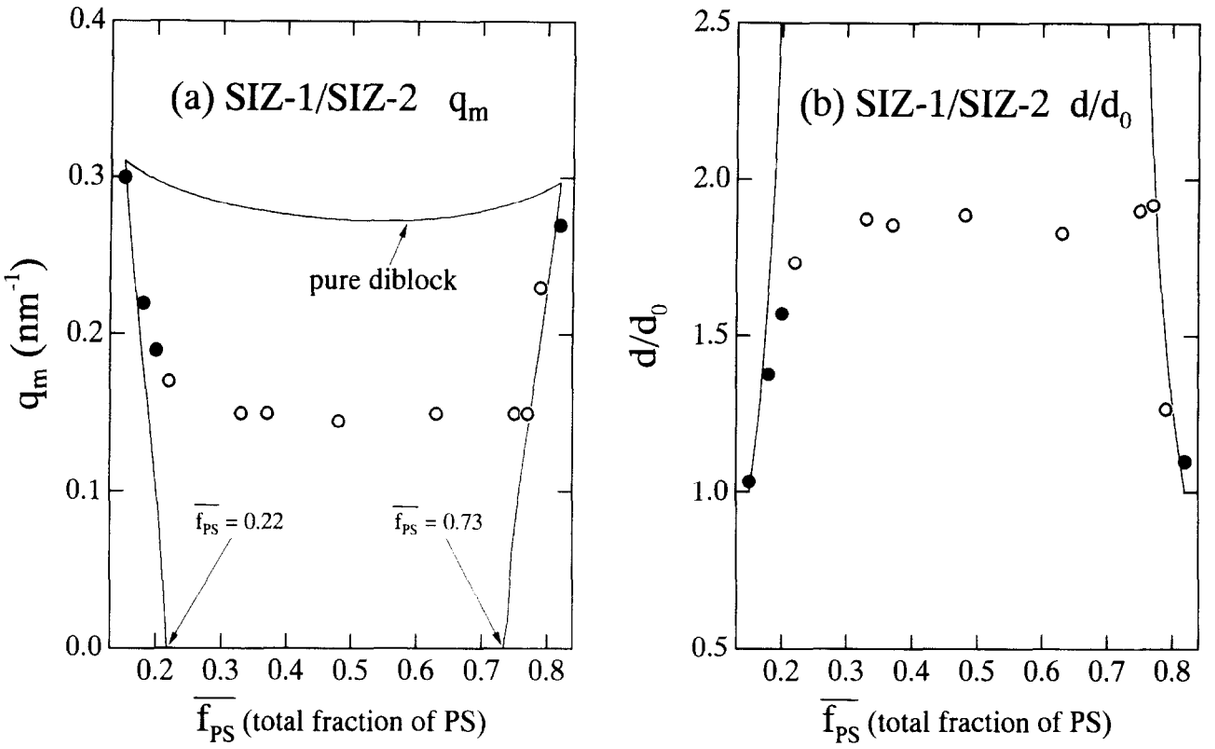

Figure 8 (a) Comparison between the theoretically predicted q_m and the experimental results of the q value of the first-order peak, as a function of the total average volume fraction of polystyrene, $\overline{f_{PS}}$. The experimental results were obtained by the small-angle X-ray scattering (SAXS) measurements at the room temperature on the toluene solution-cast films of the blends of SIZ-1 [$M_n = 4.60 \times 10^4$, $M_w/M_n = 1.09$, f_{PS} (volume fraction of polystyrene) = 0.15] and SIZ-2 ($M_n = 4.62 \times 10^4$, $M_w/M_n = 1.07$, $f_{PS} = 0.82$‡). The open circles indicate the samples macroscopically phase separated. (b) Comparison between the theoretically predicted d/d_0 and the experimental results for the normalized domain spacing (divided by d_0). The open circles indicate the samples macroscopically phase separated

local A fraction is almost 0.5, although it fluctuates. This induces lamellar structures with inhomogeneous lamellar thicknesses in the direction normal to the interface. That is, the thicknesses of lamellae may fluctuate spatially corresponding to the concentration fluctuation in ϕ_α.

The cases I and II correspond to macrophase separation. Thus, macrophase separation can occur in the vicinity of $f_A^\alpha = f_{A,crit}^\alpha$ even for the parameter regions where the macrophase separation is not explicitly predicted. Recently, we obtained experimental support for this indication[28]. *Figure 8a* shows the comparison between the theoretically predicted q_m and the experimental results of the q value of the first-order peak, as a function of the total average volume fraction of polystyrene, $\overline{f_{PS}}$. The experimental results were obtained by small-angle X-ray scattering (SAXS) measurements at room temperature on toluene solution-cast films of SIZ-1 ($M_n = 4.60 \times 10^4$, $M_w/M_n = 1.09$, f_{PS} (volume fraction of polystyrene) = 0.15) and SIZ-2 ($M_n = 4.62 \times 10^4$, $M_w/M_n = 1.07$, $f_{PS} = 0.82$‡) blends. The open circles indicate the samples macroscopically phase separated. As can be clearly seen, the agreement is good for the regions of $\overline{f_{PS}} \lesssim 0.22$ and $\overline{f_{PS}} \gtrsim 0.73$. However, in the vicinity of $\overline{f_{PS}} = 0.22$ and $\overline{f_{PS}} = 0.73$, q_m does not go down to zero. This means that the samples were already macroscopically phase separated even if the theory predicted the preferential microphase separation, as shown in *Figure 7*. Macrophase separation was actually observed for the samples with $\overline{f_{PS}} = 0.75$ and 0.77. For $0.22 \lesssim \overline{f_{PS}} \lesssim 0.73$ where macrophase separation is predicted theoretically, the q_m value remains constant at 0.15 nm^{-1}. Although the exact phase structures were not examined for those samples, the macrophase separation might induce the microphase separation with the unit size independent of the mixing ratio, i.e. $\overline{f_{PS}}$. *Figure 8b* shows the comparison between the theoretically predicted d/d_0 and the experimental results for the normalized domain spacing (divided by d_0). The values of d/d_0 are *ca* 1.9 for $0.33 \lesssim \overline{f_{PS}} \lesssim 0.73$, although those blend samples were macrophase separated. This is a clear signature of the formation of the larger size microdomains as compared to the structures of the pure components.

In order to explain the formation of the larger-size lamellar microdomains, we consider first the formation of the phase structures from the concentration fluctuation with a microscopic wavelength which is comparable to the chain dimensions of the diblocks. As illustrated in the left-hand side of *Figure 9*, the alternating arrangement of the α and β chains is most probable because it stabilizes flat interfaces for the lamellar structures. The alternating arrangement of the short and long chains in the respective microdomain may let the short chains stretch and the long chains shrink in the direction normal to the interface, as compared to the unperturbed chain dimensions. This is simply because those chains have to

‡ The values of molecular weights indicated here were obtained by g.p.c. with low-angle light scattering. After acceptance of the revised manuscript, we conducted measurements of M_n again with the membrane osmometry. More accurate values are therefore found to be 37.3 and 44.8 $\times 10^3$ for SIZ-1 and 2, respectively[29]. Accordingly, the f_{PS} values were changed slightly to 0.14 and 0.81, respectively. Nevertheless, we let the previous values remain as they are, because *Figure 8* depicts results obtained using those values.

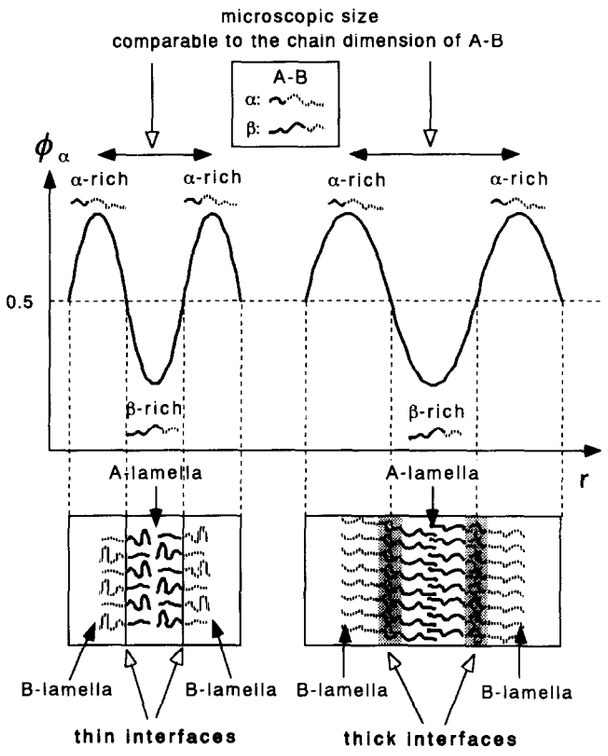

Figure 9 Schematic illustrations for the concentration fluctuation with a microscopic wavelength and for the phase structures formed upon the disorder-to-order transition. Note that the wavelength is comparable to the chain dimensions of the α- or β-blocks. ϕ_α is the fraction of the α component. The alternating arrangement of the α and β chains is sketched on the left-hand side. The alternating arrangement of the short and long chains in the respective microdomain may let the short chains stretch and the long chains shrink in the direction normal to the interface, as compared to the unperturbed chain dimensions. For a larger wavelength of the dominant concentration fluctuation, the possible model for the resultant larger lamellar structures formed upon the ODT are illustrated on the right-hand side, where the shaded regions are the thick interfaces which comprise miscible shorter A and B chains from the α and β diblocks, respectively. By arranging the α and β diblocks as shown, the adjacent longer A (or B) chains get closer so that the chains can be more stretched in the direction normal to the interface to fill up the larger lamellar space (*virtual diblock approximation*)

fill up cavities which would appear when those chains would be at the unperturbed state. It is noted again that the long chains tend to shrink as compared to the unperturbed state, with the model in the left-hand side. Even if the size of the fluctuation is larger than that in the left-hand side, the mixture may form homogeneous lamellar structures with the larger lamellar thickness. Such lamellar structures are illustrated in the right-hand side of *Figure 9*, where the shaded regions are the thick interfaces which comprise miscible shorter A and B chains from the α and β diblocks, respectively. By arranging the α and β diblocks as illustrated, the adjacent longer A (or B) chains get closer so that the chains can be more stretched in the direction normal to the interface to fill up the larger lamellar space. Thus, the molecular picture is similar to a longer diblock comprising a pair of the longer A(β) and B(α) chains. Namely, we can approximate the situation to that with a pure A(β)-*block*-B(α) diblock (*virtual diblock approximation*). Since this model assumes that those shorter A and B chains are miscible, it can be only applied to the weak segregation regime. As the segregation increases, the interfaces become thinner so that the structural image changes from the model in the right-hand side to that in the left-hand side. This means that the domain size becomes smaller as the segregation increases. This is an anomalous behaviour. However, our recent experimental results for the SIZ-1/SIZ-2 blends clearly show such anomalous behaviour[29], and also the theoretical result of Shi and Noolandi[15] confirms this behaviour. Thus, the model illustrated in the right-hand side can provide an appropriate explanation for the larger-size lamellar microdomains.

Finally, we discuss what extent the larger-size lamellar microdomains, which are predicted to appear upon the ODT, can be stabilized by the molecular arrangements of the α and β chains, like the model illustrated on the right-hand side in *Figure 9* (*virtual diblock approximation*). According to the model, the domain size in the direction normal to the interface is ascribed to the contributions of the longer A(β) and B(α) chains. Considering the structures just formed upon the ODT, no chain stretching can be assumed. Then, the total domain size, d_m, may be expressed by rescaling the wavelength of the dominant concentration fluctuation in the pure component, d_0, as:

$$d_m = d_0\left(\frac{N_{A(\beta)} + N_{B(\alpha)}}{N}\right)^{1/2} \tag{19}$$

where N is the total degree of polymerization of the α or β diblock ($N_\alpha = N_\beta = 1000$), and $N_{A(\beta)}$ and $N_{B(\alpha)}$ denote the degrees of polymerization of the A(β) and B(α) chains, respectively. *Figure 10* shows the comparisons of d/d_m with d/d_0 which is the same as plotted in *Figure 5*. The full curves are for d/d_m and the broken curves are for d/d_0. *Figure 10b* is the enlarged view. In part (*a*), it is clearly seen that the values of d/d_m are always smaller than those of d/d_0 at a fixed value of f_A^α. The values of d/d_m can be less than unity, as shown in part (*b*). Note that the values of d/d_0 can never go below unity. These facts indicate that the larger-size lamellae, which are thought to be hard for the ($\alpha + \beta$) mixtures to maintain, can be stabilized by arranging those chains as illustrated in the right-hand side of *Figure 9*. Thus, the model with the thick interfaces is informative to the phase structures in the weak segregation regime for the binary mixtures of compositionally asymmetric diblocks.

CONCLUSIONS

Random phase approximation (RPA) calculations were conducted for the binary mixtures of diblock copolymers, α: $(A-B)_1$ and β: $(A-B)_2$ to calculate the scattering functions and to analyse the stability of the mixtures. The parameter values used for the simulations are that the total degree of polymerization, $N(=N_\alpha = N_\beta)$, is 1000, the radius of gyration, $R_g(=R_{g,\alpha} = R_{g,\beta})$, is 10 nm, the inhomogeneity index of molecular weight, M_w/M_n, is in the range of 1.0–1.5, and the segmental volume, $v_A = v_B = 100\,cm^3\,mol^{-1}$. The fraction of A in $\alpha(f_A^\alpha)$ and that in $\beta(f_A^\beta)$ are varied in such a way that they satisfy $f_A^\alpha + f_A^\beta = 1$. As a result, it is predicted that the homogeneous mixture undergoes microphase separation as the segregation increases, for f_A^α larger than a particular value $(f_{A,crit}^\alpha)$ which is dependent on the values of M_w/M_n. On the other hand, for $f_A^\alpha < f_{A,crit}^\alpha$ the macroscopic phase separation between α and β is expected to occur prior to the microphase separation. It is also found that the wave-length of the dominant concentration fluctuation in the homogeneous mixture gradually increases as f_A^α

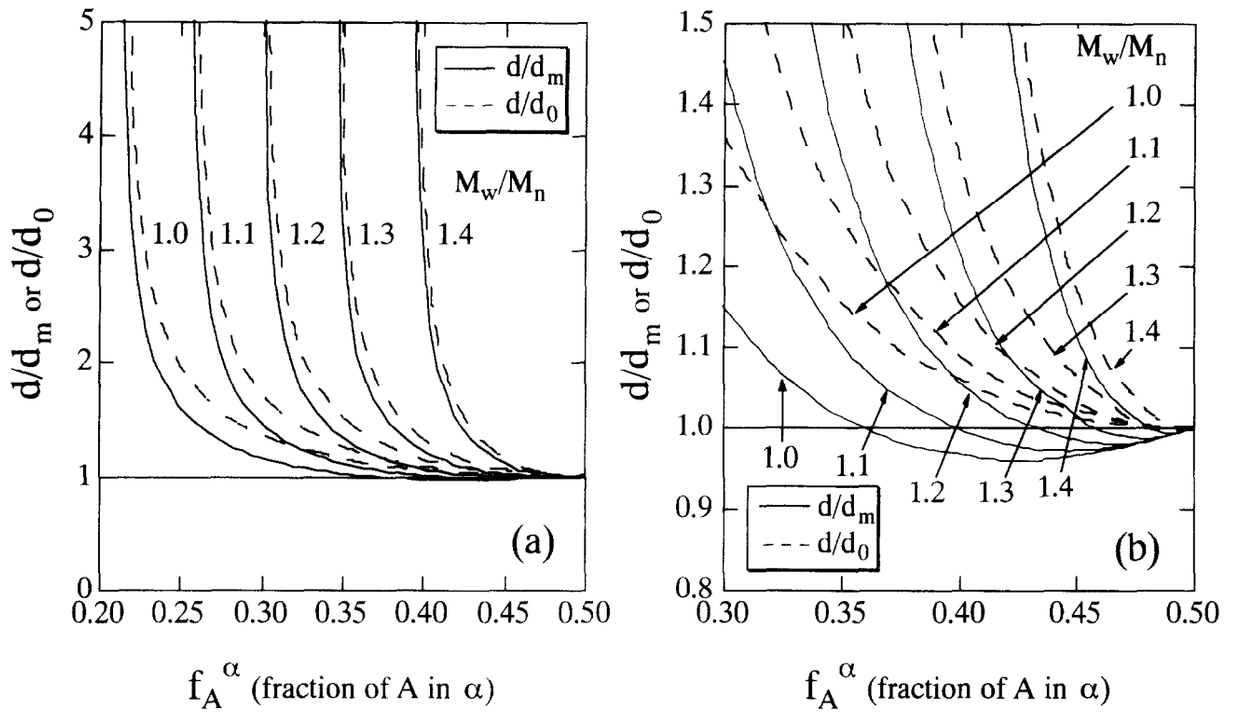

Figure 10 (a) Comparisons of d/d_m with d/d_0 which is the same as plotted in *Figure 5*. Here, d_m denotes the total domain size obtained by rescaling d_0 as expressed by eq (19). The full curves are for d/d_m and the broken curves are for d/d_0. (b) Enlarged view of the plots in the part (a) in the region of $0.8 \leq (d/d_m \text{ or } d/d_0) \leq 1.5$ and $0.3 \leq f_A^\alpha \leq 0.5$

approaches $f_{A,crit}^\alpha$ from the upper side of f_A^α. At $f_A^\alpha = f_{A,crit}^\alpha$, the wavelength diverges, indicating macrophase separation. These results give some implications to the unit size of the microdomains formed upon the ODT for $f_A^\alpha > f_{A,crit}^\alpha$. Namely, the unit size might be larger than those of the component pure diblocks. Finally, the phase diagram is examined for the binary mixtures of the diblock copolymers to demonstrate how it is different from the phase diagram of the pure block copolymer. The disagreement in the ODT spinodal lines between the pure block copolymers and the binary mixtures is pronounced in almost the entire region of the total fraction of A ($\overline{f_A}$) besides the vicinity of $\overline{f_A} = f_A^\alpha$ or $\overline{f_A} = f_A^\beta$. This should be noted in the experiments, for example in the case of the study of the composition dependence of the interaction parameter. That is, the binary mixture cannot provide a conventional way as an alternative to the pure block copolymer. In other words, the results for the composition dependence of the interaction parameter χ evaluated from the $(\alpha + \beta)$ mixtures may be different from those of the pure block copolymers.

ACKNOWLEDGEMENTS

This work is supported in part with a Grant-in-Aid from Japan Ministry of Education, Science, Culture and Sports with 07236228 granted to S. N. (Priority Areas 'Cooperative Phenomena in Complex Liquids') and 08751048 granted to S. S.

REFERENCES

1. Sakurai, S., *Trends Polym. Sci.*, 1995, **3**, 90, and refs therein.
2. Hashimoto, T., Tanaka, H. and Hasegawa, H. in *Molecular Conformation and Dynamics of Macromolecules in Condensed Systems*, ed. M. Nagasawa. Elsevier, Tokyo, p. 257, 1988.
3. Tanaka, H., Hasegawa, H. and Hashimoto, T., *Macromolecules*, 1991, **24**, 240.
4. Hashimoto, T., Kimishima, K. and Hasegawa, H., *Macromolecules*, 1991, **24**, 5704.
5. Winey, K. I., Thomas, E. L. and Fetters, L. J., *Macromolecules*, 1992, **25**, 2645.
6. Spontak, R. J., Smith, S. D. and Ashraf, A., *Macromolecules*, 1993, **26**, 5118.
7. Lowenhaupt, B., Steurer, A., Hellmann, G. P. and Gallot, Y., *Macromolecules*, 1994, **27**, 908.
8. Hashimoto, T., Koizumi, S. and Hasegawa, H., *Macromolecules*, 1994, **27**, 1562.
9. Hashimoto, T., Tanaka, H. and Hasegawa, H., *Macromolecules*, 1990, **23**, 4378.
10. Hadziioannou, G. and Skoulios, A., *Macromolecules*, 1982, **15**, 267.
11. Hashimoto, T., Yamasaki, K., Koizumi, S. and Hasegawa, H., *Macromolecules*, 1993, **26**, 2895.
12. Hashimoto, T., Koizumi, S. and Hasegawa, H., *Macromolecules*, 1994, **27**, 1562.
13. Koizumi, S., Hasegawa, H. and Hashimoto, T., *Macromolecules*, 1994, **27**, 4371.
14. Shi, A.-C. and Noolandi, J., *Macromolecules*, 1994, **27**, 2936.
15. Shi, A.-C. and Noolandi, J., *Macromolecules*, 1995, **28**, 3103.
16. Spontak, R. J., *Macromolecules*, 1994, **27**, 6363.
17. Matsen, M. W., *J. Chem. Phys.*, 1995, **103**, 3268.
18. Matsen, M. W. and Bates, F. S., *Macromolecules*, 1995, **28**, 7298.
19. Zhao, J., Majumdar, B., Schulz, M. F., Bates, F. S., Almdal, K., Mortensen, K., Hajduk, D. A. and Gruner, S. M., *Macromolecules*, 1996, **29**, 1204.
20. Leibler, L., *Macromolecules*, 1980, **13**, 1602.
21. de Gennes, P.-G., *Scaling Concepts in Polymer Physics*. Cornell University Press, Ithaca, NY, 1979.
22. Tanaka, H. and Hashimoto, T., *Polym. Commun.*, 1988, **29**, 212.
23. Schultz, G. V., *Z. Phys. Chem.*, 1939, **B43**, 25.
24. Zimm, B. H., *J. Chem. Phys.*, 1948, **16**, 1099.
25. Leibler, L. and Benoit, H., *Polymer*, 1981, **22**, 195.
26. Bate, F. S. and Hartney, M. A., *Macromolecules*, 1985, **18**, 2478.
27. Mori, K., Tanaka, H., Hasegawa, H. and Hashimoto, T., *Polymer*, 1989, **30**, 1389.
28. Sakurai, S., Irie, H. and Nomura, S. in preparation.
29. Sakurai, S., Umeda, H., Yoshida, A. and Nomura, S. *Macromoles*, submitted.